International Journal of Microwave and Wireless Technologies

cambridge.org/mrf

Design of a flexible ultra-wideband antenna with six band-notched characteristics for wearable applications

Chengzhu Du and Tianshi Wang

School of Electronics and Information Engineering, Shanghai University of Eletric Power, Shanghai, People's Republic of China

Research Paper

Cite this article: Du C, Wang T (2025) Design of a flexible ultra-wideband antenna with six band-notched characteristics for wearable applications. *International Journal of Microwave and Wireless Technologies* **17**(1), 74–82. https://doi.org/10.1017/S1759078724001387

Received: 13 March 2024
Revised: 9 December 2024
Accepted: 11 December 2024

Keywords:
liquid crystal polymer; notch band; splitted concentric ring; UWB; wearable antenna

Corresponding author: Chengzhu Du; Email: duchengzhu@163.com

Abstract

This paper proposes a compact coplanar waveguide-fed slot antenna for ultra-wideband wearable applications, featuring six notch bands. The antenna utilizes a flexible liquid crystal polymer substrate with a thickness of 0.1 mm. The antenna achieves six band-notched characteristics by incorporating a split concentric ring etched on the radiating patch and L-shaped branches loaded on the ground plane. The proposed flexible antenna has dimensions of 30×30 mm^2($0.65\lambda_0$*$0.65\lambda_0$, $\lambda 0$ is the free space wavelength at 6.5 GHz.). Measurement results show an impedance bandwidth ranging from 2.37 to 13.7 GHz and a fractional bandwidth of 134%. The notch bands cover 2.9–3.77 GHz for WiMAX applications, 4.14–4.9 GHz for the ARN band, 5.09–5.55 GHz for the WLAN downlink band, 5.86–6.46 GHz for the C-band uplink band, 6.66–7.39 GHz for the C-band/INSAT/super-extended band, and 7.93–8.43 GHz for ITU-8 GHz. The maximum gain in the operating band is 6.5 dBi. The performances of the flexible antenna are analyzed under bending conditions. The ANSYS HFSS electromagnetic simulator was used for the design and simulation of the proposed antenna. The flexible antenna is suitable for wearable applications.

Introduction

Ultra-wideband (UWB) technology, a method of wireless communication method functioning within the frequency range of 3.1–10.6 GHz, has garnered substantial interest in recent times given the increasing need for swift wireless communication systems. The Federal Communications Commission (FCC) approved this frequency band for commercial usage in 2002. UWB technology is associated with several benefits, including impressive data transfer speeds, efficient power usage, and robust resistance to interference [1]. However, designing a UWB antenna with consistent and predictable performance across the entire band is a challenging task. The antenna must also have high radiation efficiency and be able to accommodate the UWB bandwidth. In addition, UWB antenna featuring notched bands is popular in many applications, which can avoid interference with other narrowband services such as WLAN, WiMAX, and X-band satellite communication [2].

There are many methods for producing multi-band notch bands in UWB antennas [3–14], including etching a splitted concentric ring (SCR) on the radiating element [3, 4, 6, 7, 11, 13, 14], loading slot and parasitic branches on the antenna [5, 8, 9, 12], embedding electromagnetic band gap (EBG) structures on the ground plane [10]. The abovementioned antennas have no more than five notched bands in the designed operating frequency band, and it is still challenging to design more notched bands in a small size antenna.

At the same time, wearable antennas have received widespread attention for its revolutionary potential in the fields of communications, health monitoring, and medical applications [11–18]. In Chilukuri and Gogikar [11], the wearable textile antenna is designed on two different dielectric substrate, which show that the antenna has an impedance bandwidth of 1.8–10 GHz with two notched bands. In Roy and Nandi [12], a flexible and wearable UWB antenna based on jeans substrate is proposed. The antenna shows the operating frequency ranges ($S11 \leq -10$ dB) in 2.4–4.2 GHz and 5.86–10.7 GHz bands with notch properties in telemetry/mobile communications (4.4–4.99 GHz) and WLAN (5.15–5.85 GHz) band. In Rahmatian et al. [13], a planar full-ground plane UWB antenna based on PDMS substrate is presented with ability to reject C band (6.3–7.15 GHz) using split ring slots. In Zhao et al. [14], a miniaturized wearable antenna is proposed with five notched features, covering the entire UWB spectrum from 2.56 GHz to 12.7 GHz. In Lee and Park [15], a flexible wideband antenna operating in WLAN/c band /x band is designed. In Chengzhu et al. [17], an ultra-thin CPW-fed ultra-wideband flexible MIMO antenna for Internet of Things (IoT) applications is proposed, covering the entire spectrum from

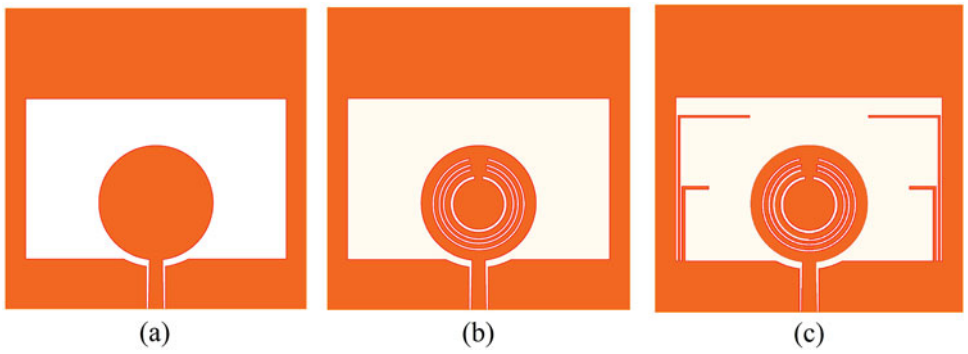

Figure 1. The design process of the antenna. (a) Antenna a, (b) Antenna b and (c) Antenna c.

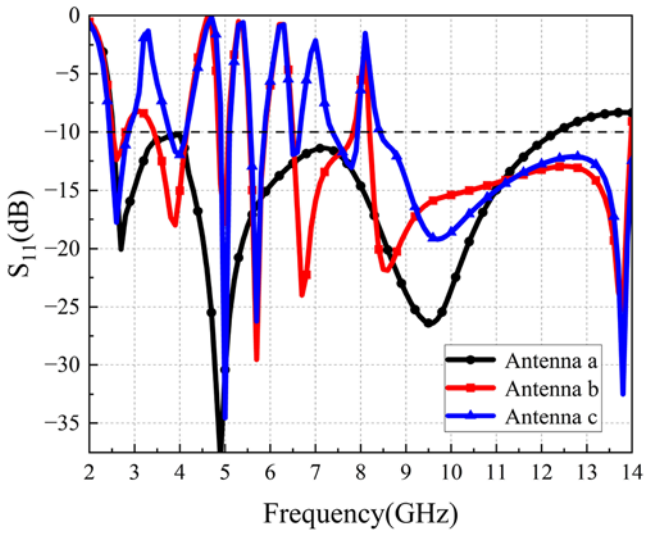

Figure 2. The S_{11} of the Antenna a, Antenna b and Antenna c.

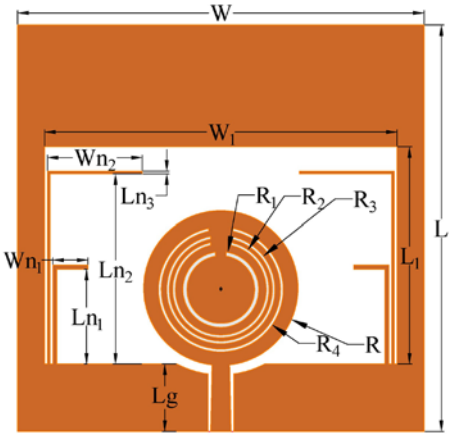

Figure 3. The geometry of the ultra-wideband antenna with six band-notched characteristics.

4.4 GHz to 39.2 GHz. In Wang et al. [18], a compact coplanar waveguide (CPW) fed wearable slot antenna with four notched bands for ultra-wideband (UWB) applications is presented, and the impedance bandwidth of the measured antenna ranges from 2.46 GHz to 12.52 GHz.

Table 1. Optimized design parameters of the antenna

Parameter	Value (mm)	Parameter	Value (mm)	Parameter	Value (mm)
W	30	L	30	Lg	5
W_1	26	Ln_1	7	R	5.7
Wn_1	2.6	Ln_2	14	R_1	2.5
Wn_2	7	Ln_3	0.2	R_2	3.36
R_3	3.8	R_4	4.4	L_1	16

Various flexible substrate materials such as Fleece, Perspex, Plastic materials, Cotton, Rogers Duroid RO3003™ (semi-flexible), Polyurethane, Jeans, etc., are commonly used as substrates in wearable antennas. Different flexible materials have different properties, so the choice of substrate is particularly important. Liquid crystal polymer (LCP), as an innovative substrate material, has the advantages of low dielectric loss, minimum coefficient of thermal expansion and cost effectiveness, and is the preferred material for flexible antenna design [19–21]. The water absorption of LCP is very low, only 0.04%, reducing the risk of relative dielectric constant and loss of tangential changes. In addition, LCP has significant chemical resistance, high-dimensional stability, and excellent mechanical strength, further improving its applicability in demanding applications in antenna technology. This quality makes it ideal for compact, high-performance devices and holds great promise in wearable applications. For the above reasons, LCP substrate material is chosen as the medium base in this paper.

This paper introduces a wearable antenna which offers six band-notched characteristics. The innovation points of the proposed antenna include [1]: The compact antenna has six notched bands [2]. The antenna is flexible, making it suitable for applications on the human body [3]. The slotted antenna has wider impedance bandwidth [4]. Using coplanar waveguide (CPW) feeding, the antenna can be used in microwave integrated circuits easily.

Section II specifies the flexible six notched-band antenna design process and its performance. Section III presents the antenna design followed by its results and discussion including S parameters, surface currents, far radiation pattern, peak gain, bending analysis, and on-body effects. Finally, Section V summarizes the work.

https://doi.org/10.1017/S1759078724001387 Published online by Cambridge University Press

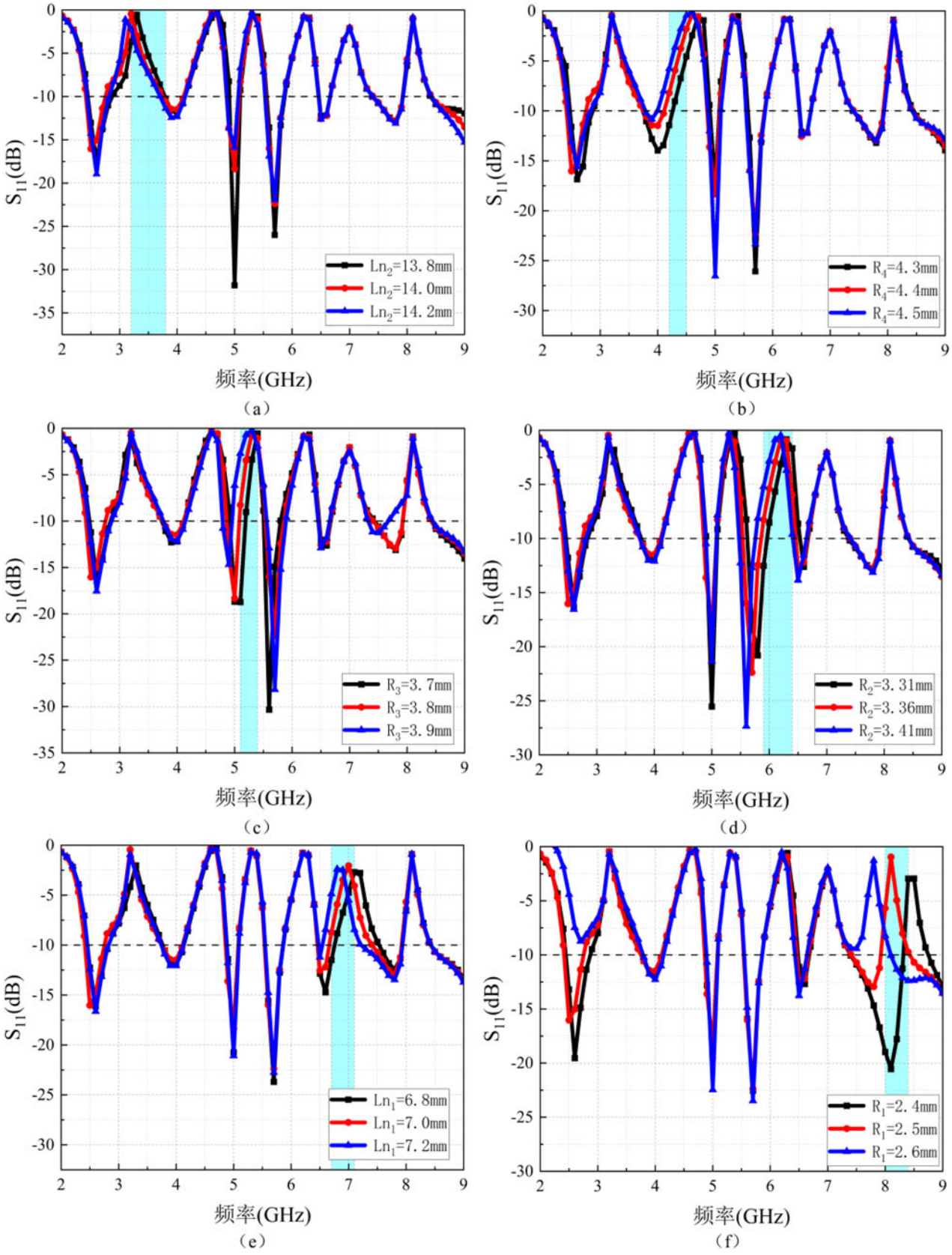

Figure 4. Parametric analysis of the notched frequency bands (a) Ln_2, (b) R_4 , (c) R_3 , (d) R_2 , (e) Ln_1 and (f) R_1.

https://doi.org/10.1017/S1759078724001387 Published online by Cambridge University Press

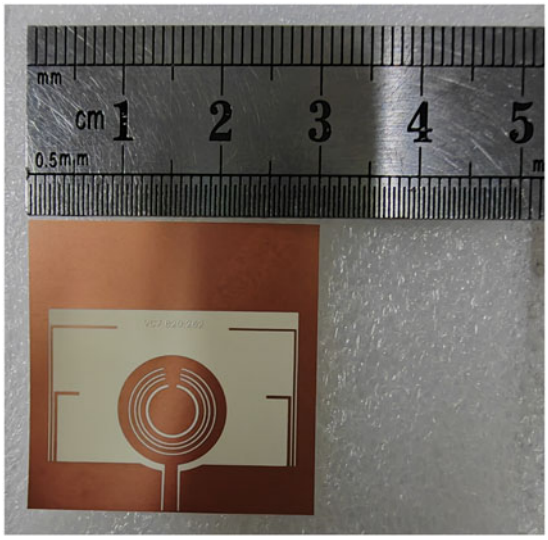

Figure 5. The geometry of the ultra-wideband antenna with six band-notched characteristics.

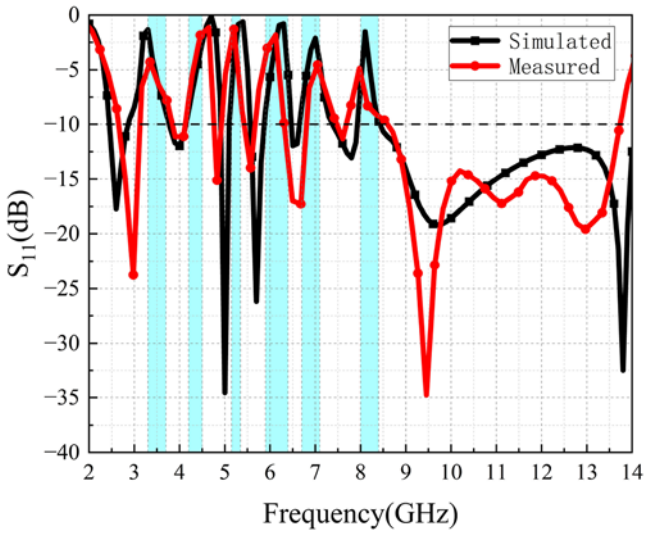

Figure 6. The S_{11} of the proposed UWB antenna with six band-notched characteristics.

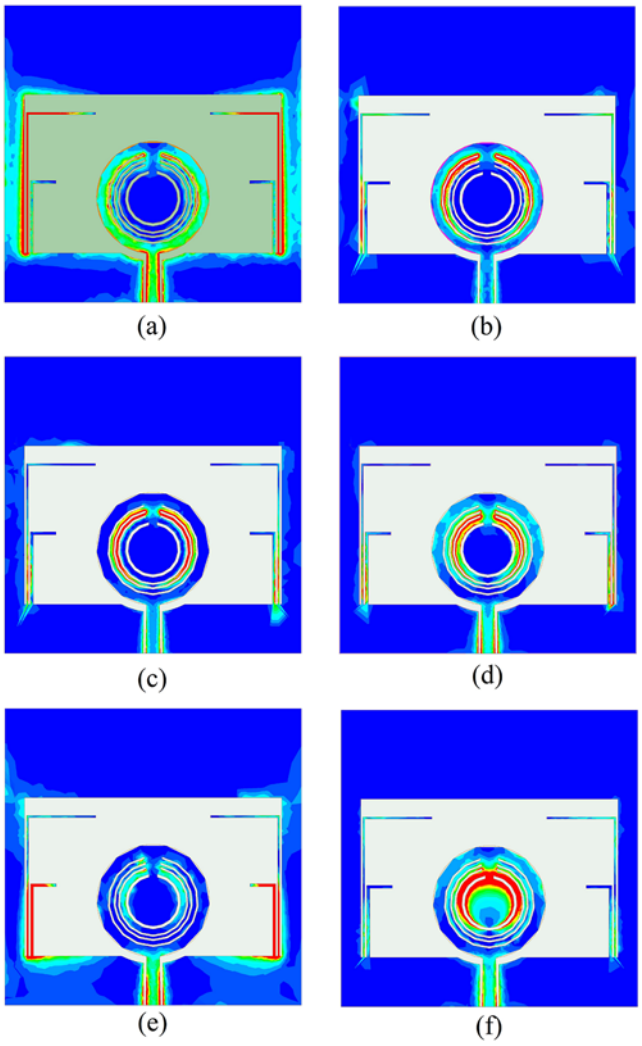

Figure 7. The distribution of surface currents on the antenna at (a) 3.2GHz, (b) 4.6GHz, (c) 5.3GHz, (d) 6.2GHz, (e) 7GHz, and (f) 8.1GHz.

Antenna design

Antenna design process

The design evolution of the antenna is shown in Fig. 1, and the S-parameters during the design process are displayed in Fig. 2.

Firstly, Antenna a is the first design step, the antenna covers the entire ultra-wide band frequency range with a bandwidth of 2.52–12.3 GHz, and the antenna uses CPW feeding. In this antenna design, a circular patch with a radius of 5.7 mm is used, and slots are etched on both sides of the ground plane of the feed line, and the feed line size is gradually tapered to achieve better impedance matching characteristics.

Secondly, Antenna b is the second design step, the antenna with four band-notched characteristics is designed by etching four differently sized stepped impedance resonators (SCRs) on a circular radiation patch of the UWB antenna. Each SCR can generate a notch band, resulting in four band-notched characteristics. The SCRs are located at the center of the radiation patch, and the position and size of the gap and radius of each SCR can be adjusted to the generated relational notch band. The simulated results of Antenna b show that the bandwidth range with S_{11} <−10 dB is achieved from 2.51 GHz to 13.99 GHz. The notches of the Antenna b are located at 4.15–4.85 GHz, 5.08–5.54 GHz, 5.89–6.5 GHz, and 7.83–8.2 GHz.

Finally, Antenna c is the third design step, on the basis of the Antenna b with four band-notched characteristics, two L-shaped branches were added to each side of the ground plane, resulting in Antenna c with six band-notched characteristics. It can be easily seen that two additional notch bands are generated without interfering with the other four notch bands, and the modifications of the antenna structure are not needed. At this point, the simulated results of Antenna c show that the bandwidth range with S_{11} <−10 dB is from 2.43 GHz to 14.01 GHz. The notches of the Antenna c are located at 2.9–3.77 GHz, 4.14–4.9 GHz, 5.09–5.55 GHz, 5.86–6.46 GHz, 6.66–7.39 GHz, and 7.93-8.43 GHz.

Figure 3 illustrates the geometry of the ultra-wideband antenna featuring six band-notched characteristics. The antenna utilizes an

https://doi.org/10.1017/S1759078724001387 Published online by Cambridge University Press

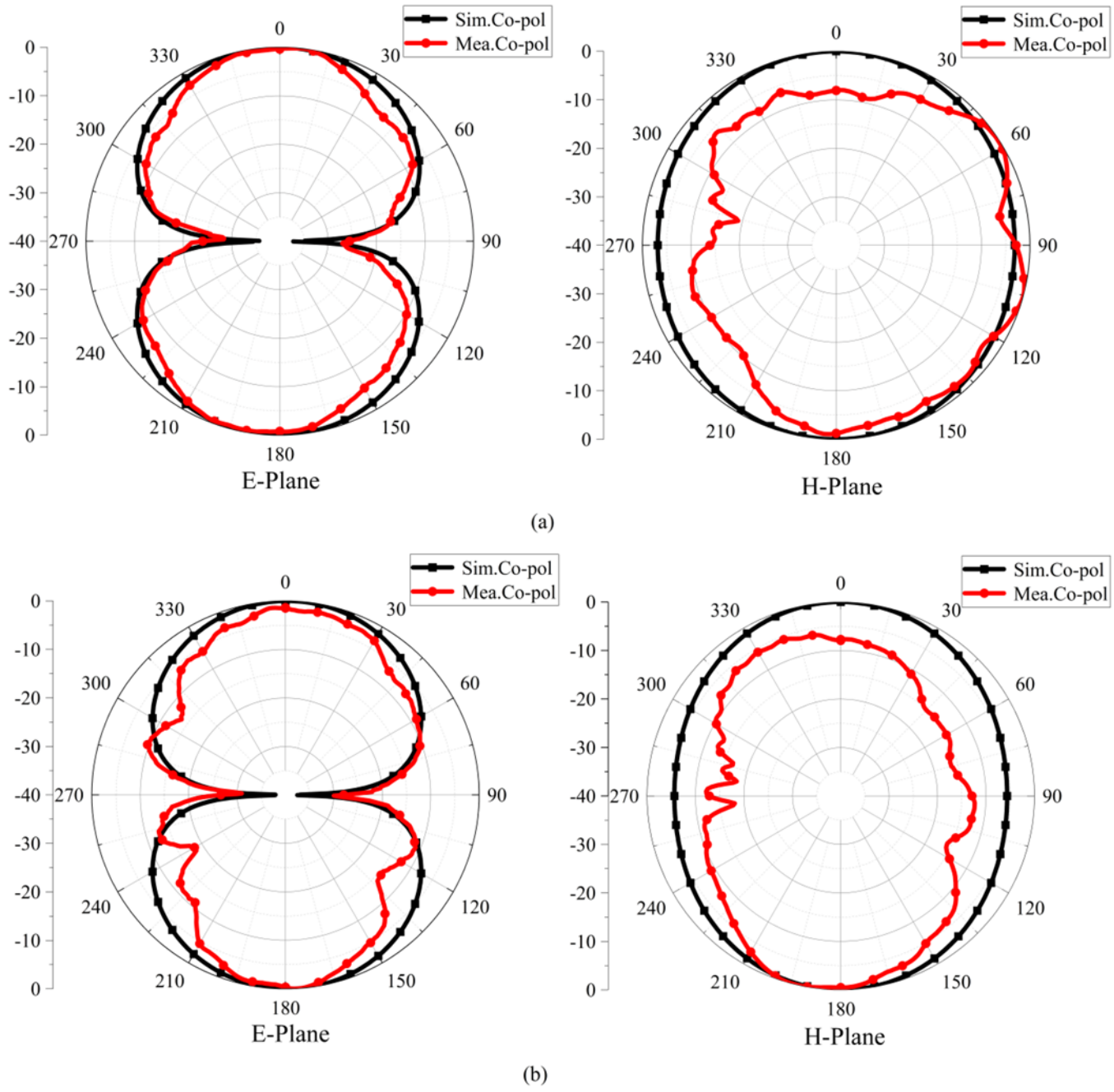

Figure 8. The simulated and measured E-Plane and H-Plane radiation patterns. (a) 2.5GHz and (b) 5GHz.

LCP dielectric substrate with specific properties, including a relative dielectric constant of 2.9, a loss tangent (tan δ) of 0.002, a thickness of 0.1 mm, and a CPW feed. The antenna design comprises a circular patch as the primary radiating element, along with an enhanced coplanar ground structure. The optimized parameters obtained through the use of HFSS software optimization are presented in Table 1.

Parametric analysis of the notched frequency bands

By analyzing the parameters of each notched band, it is evident that effective control over the notched bands can be achieved by adjusting the length of the L-shaped stubs and the radius of the SCRs. The first notched band can be controlled by adjusting the length Ln2 of the longer L-shaped stub, as shown in Fig. 4(a). The second notched band can be controlled by adjusting the radius R4 of the SCR, as shown in Fig. 4(b). The third notched band is controlled by the radius R3 of the SCR, as shown in Fig. 4(c). The fourth notched band is managed by adjusting the radius R2 of the SCR, as shown in Fig. 4(d). The fifth notched band can be controlled by the length Ln1 of the shorter L-shaped stub, as shown in Fig. 4(e). The sixth notched band can be adjusted by varying the radius R1, as shown in Fig. 4(f). These figures demonstrate that each notched band can be

https://doi.org/10.1017/S1759078724001387 Published online by Cambridge University Press

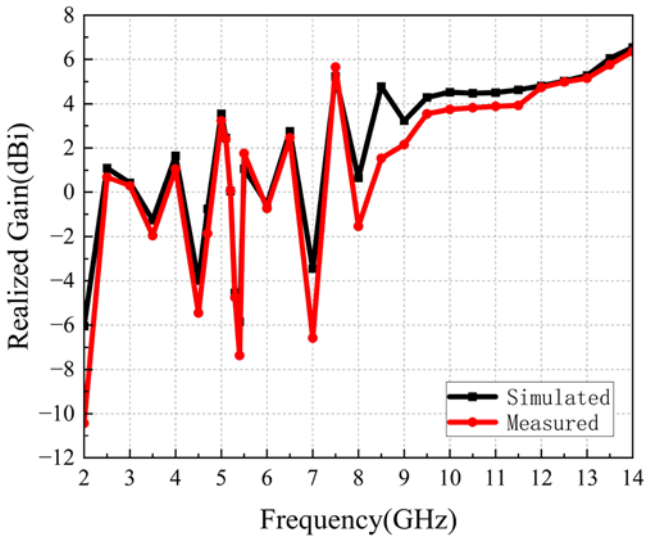

Figure 9. The measured and simulated realized gain.

individually controlled with minimal impact on the other notched bands.

Results and discussions

Simulated and measured s-parameter

The performance of the proposed antenna was simulated using HFSS software, and the results were clearly displayed. Figure 5 shows the actual processing diagram of the antenna. Figure 6 also shows the reflection coefficient magnitudes ($|S_{11}|$) of the ultra-wideband antenna, which has six band-notched characteristics. The measured working bandwidth range with S_{11} <−10 dB is from 2.7 GHz to 13.7 GHz, and the measured notches of the antenna are located at 3.1–3.75 GHz for Wimax, 4.14–4.7 GHz for ARN, 5–5.5 GHz for WLAN, 5.7–6.38 GHz for C-band, 6.8–7.5 GHz for X-band, and 7.75–8.7 GHz for ITU-8 GHz. Each notch exhibits a peak value greater than −5 dB, signifying the outstanding notch performance of the antenna. The measured S_{11} is almost identical to the simulated S_{11}, with some differences due to manufacturing defects and the inability of the antenna testing equipment and the testing environment to reach ideal conditions during testing.

The distribution of surface currents

Figure 7 shows the distribution of surface currents on the proposed antenna at 3.2 GHz, 4.6 GHz, 5.3 GHz, 6.2 GHz, 7 GHz and 8.1 GHz. In Fig. 7(a), it can be observed that the currents are predominantly distributed along the longer L-shaped stub. In Fig. 7(b), the currents are mainly focused around the SCR with a radius of R_4. Similarly. In Fig. 7(c), the currents are mainly focused around the SCR with a radius of R_3. In Fig. 7(d), the currents are primarily focused around the SCR with a radius of R_2. In Fig. 7(e), the currents are mainly distributed along the shorter L-shaped stub, and in Fig. 7(f), the currents are mainly focused around the SCR with a radius of R_1. The current distribution shows the successful achievement of non-radiation effects of the antenna at specific frequencies.

Radiation pattern and peak gain analysis

For the designed UWB slot antenna with six band-notched characteristics, it is necessary to analyze its radiation pattern characteristics and peak gain. By selecting two representative non-notch band frequency points, 2.5 GHz and 5 GHz. we obtained the normalized radiation patterns in the E and H plane. Figure 8 presents the simulated and actual measured results of the radiation pattern. It is evident that at the frequencies of 2.5 GHz and 5 GHz. The antenna exhibits an "8" shape radiation pattern in the E-plane and omni-directional radiation in the H-plane, indicating that the antenna is suitable for receiving and transmitting signals from any direction in the working frequency band.

In addition, the simulation and measurement realized gains of the antenna are given in Fig. 9. The realized gain of the antenna sharply decreases at the notch band frequencies, and most of the notch bands achieve negative gain values, reflecting the excellent band-notched characteristics of the antenna. In other operational frequency bands, the gain surpasses 0, and the maximum gain of the antenna exceeds 6.5dBi, demonstrating that the antenna can achieve six band-notched characteristics and has satisfactory radiation characteristics in the working frequency band.

Bending analysis

In order to assess the flexibility of the antenna, we simulated its radiation characteristics while it was bent along the H-plane. The dielectric substrate utilized for the antenna is a flexible LCP material with a thickness of only 0.1 mm. In our simulation, we securely mounted the antenna on cylinders with radii of 30 mm and 50 mm, respectively, and plot the bent S_{11} curves under different curvature radii, as shown in Fig. 10. It can be found that under bending conditions, the antenna bandwidths of the two states all cover 2.7–11 GHz. When the antenna is fixed on a cylindrical surface with a radius of 50 mm, the degree of bending is relatively small, and at this time, the six notch bands can still be achieved, albeit with a certain degree of offset. When the antenna is fixed on a cylindrical surface with a radius of 30 mm, the degree of bending is relatively large, and at this time, The first and second notch bands are connected between 3 and 4 GHz, changing from six band-notched characteristics to five band-notched characteristics.

On-body effects

To investigate the characteristics of the antenna when close to the human body, we positioned the antenna on the arm, chest, and leg. The actual measured results of slot antenna on these body locations are depicted in Fig. 11. It is observed that when the antenna is closed to the human body, its bandwidth experiences a significant reduction, and the position of the notch band slightly shifts. Specifically, the first notch band moves towards lower frequencies. When the antenna is closed to the arm or the leg, it has all six complete notch bands. When the antenna is closed to the chest, the fifth and sixth notch bands are connected, so the measurement results are better on the arm and leg than on the chest.

Specific absorption rate validation

In the realm of wearable antenna applications, the quantitative assessment of the impact of antenna radiation energy on human

https://doi.org/10.1017/S1759078724001387 Published online by Cambridge University Press

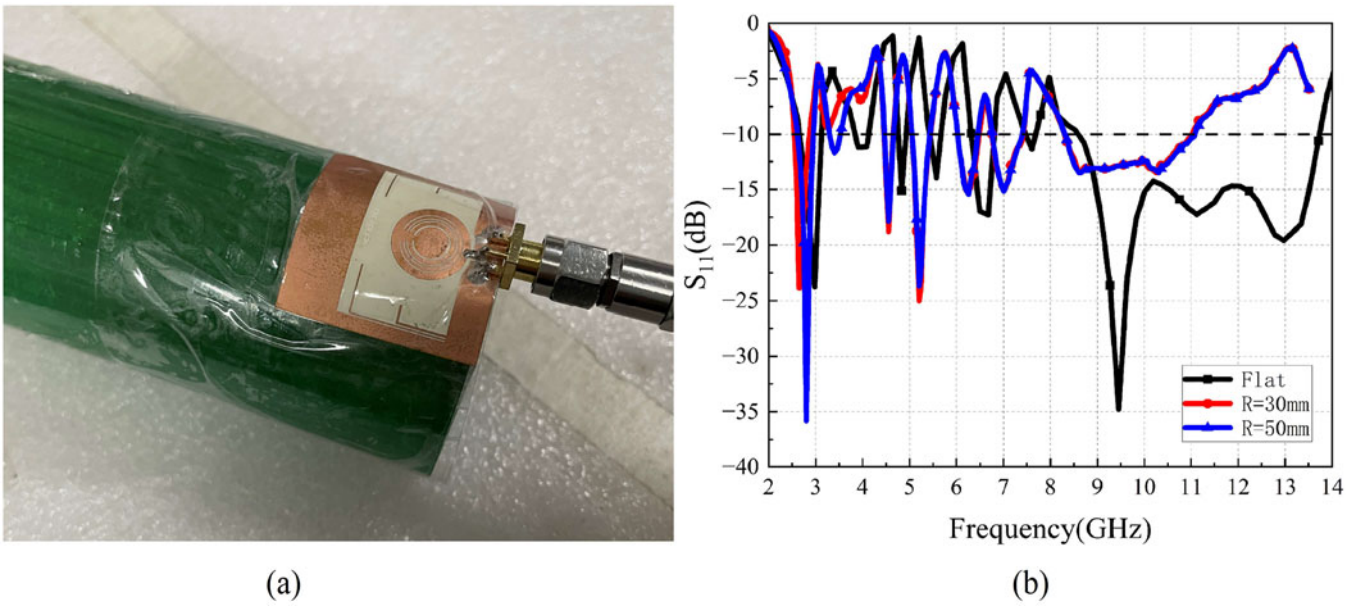

Figure 10. The S_{11} of the bending antenna. (a) Bending measurement setup and (b) the measured S_{11} of the antenna when flat and bend.

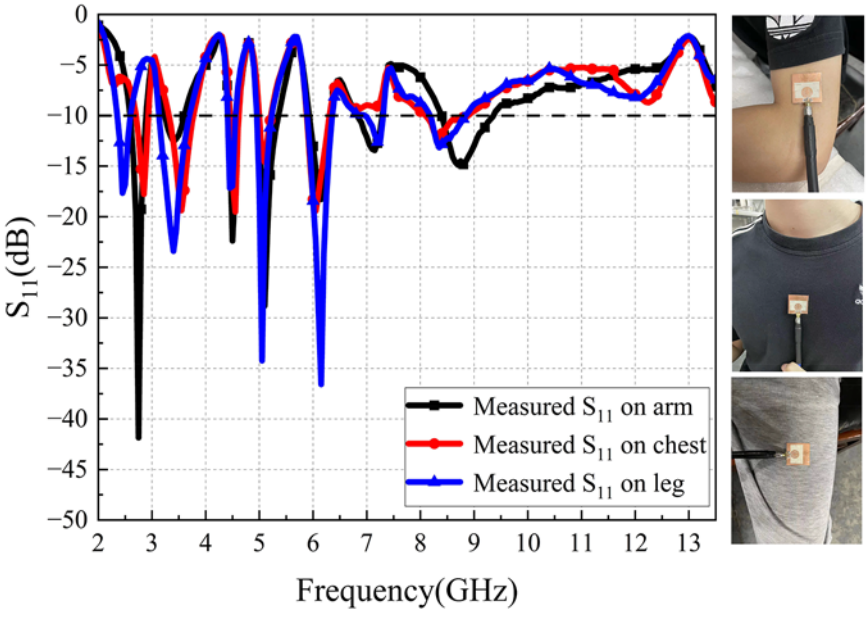

Figure 11. The measured S_{11} of the antenna placed on human body.

tissues is typically conducted through Specific Absorption Rate (SAR) measurements. The evaluation of SAR values is paramount in determining whether the antenna poses any potential radiation risks to the human body.

In the simulation, the human body model is characterized by four distinct layers: skin, fat, muscle, and bone, each with specified thicknesses—1 mm for the skin, 5 mm for fat, 20 mm for muscle, and 14 mm for bone. Collectively, the human body model possesses a total thickness of 40 mm. The separation distance between the antenna and the human tissue model is set at 5 mm, with an input power of 0.1 W. Figure 12 displays the three-dimensional distribution of SAR for the proposed antenna. SAR values were simulated in 10 g of biological tissue at frequencies of 2.5 GHz and 5 GHz. At 2.5 GHz, the maximum SAR value is 1.48 W/kg, and at 5 GHz, the maximum SAR value is 0.96 W/kg. The findings indicate that the SAR values remain below the European standard of 2 W/kg per 10 g of tissue, adhering to established guidelines for radiation exposure.

Comparison

Comparing the slot antenna with the literature referenced earlier, it can be observed for Table 2 that the slot antenna has more notch bands, smaller dimensions, wider bandwidth and higher gain. Importantly, this antenna is flexible and can be applied in the field of wearable devices.

https://doi.org/10.1017/S1759078724001387 Published online by Cambridge University Press

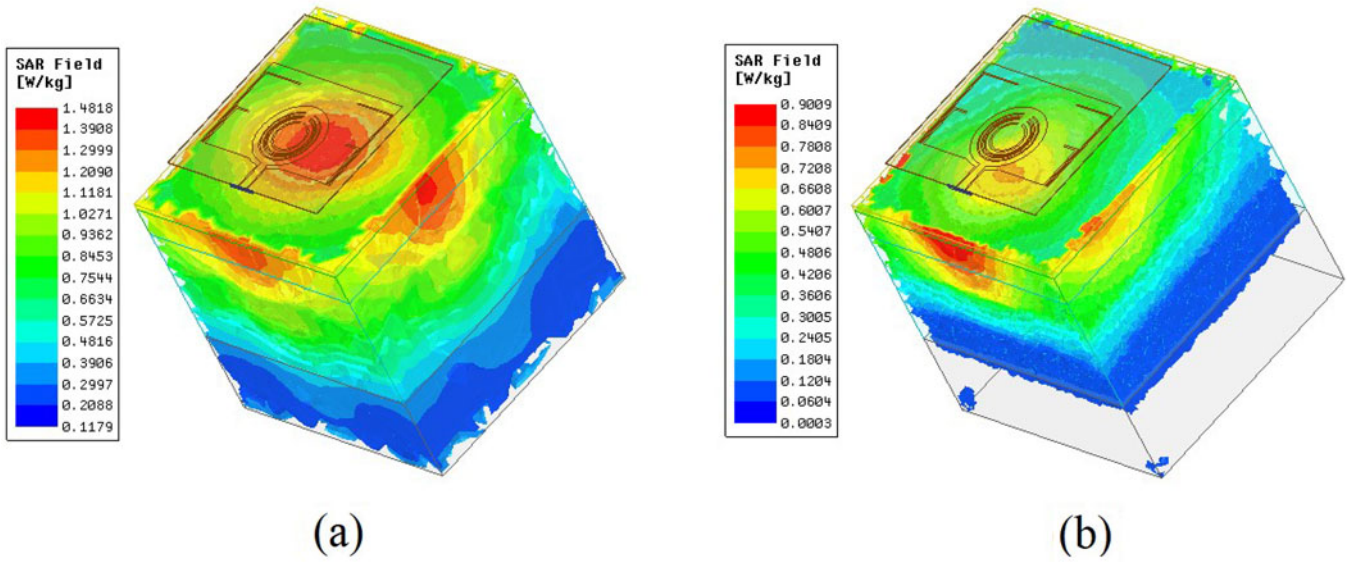

Figure 12. The SAR distribution of the antenna positioned on the human tissue at (a) 2.5 GHz and (b) 5 GHz.

Table 2. Comparison of proposed work with other literature works

Ref.	Overall size (λ_0^2)	Bandwidth (GHz)	No. of notch bands	Notching frequencies (GHz)	Max gain (dBi)	Substrate material	Flexible
[3]	0.54 × 0.65	2.4–10.6 (120%)	2	3.4–3.69, 5.15–5.85	6	FR4	Rigid
[4]	0.92 × 0.67	2.7–11.06 (128%)	3	3.22 –3.83, 4.49 –5.05, 7.49 –8.02	3.8	FR4	Rigid
[5]	0.82 × 0.75	3.1–10.6 (110%)	3	4.0–4.4, 5.2–5.8, 8.0–8.25	4.6	Rogers 5880	Semi-Flexible
[6]	0.73 × 0.56	3–11.6 (110%)	4	3.3–3.8, 5.172 –5.82, 7.2–7.7, 8.0 –8.5	5.11	RT/DUROID	Rigid
[8]	0.81 × 0.7	2.9–11 (99%)	4	3.38 –3.75, 5.01 –5.25, 5.63 –5.86, 7.45 –7.82	4	Rogers 5880	Semi-Flexible
[9]	0.61 × 0.52	4.18–13.9 (107%)	4	5.05, 7.8, 9.03, 10.86	5	FR4	Rigid
[10]	1.66 × 1.60	2.05–14 (156%)	2	2.4–3.7, 5.15–5.725	12.7	Kapton	Flexible
[11]	0.85 × 0.79	1.8–10 (142%)	2	2.3–2.5, 3.3–3.6	5.09	Denim	Flexible
[12]	0.52 × 0.86	2.4–11.25 (132%)	2	4.4–4.99, 5.15–5.85	4.8	Jeans	Flexible
[14]	0.64 × 0.76	2.56 –12.7 (133%)	5	2.58 –3.18, 4.05 –4.29, 5–5.64, 8.6–9.05, 9.2–10.32	4.76	Rogers 5880	Semi-Flexible
This work	0.65 × 0.65	2.7–13.7 (134%)	6	3.1–3.75, 4.14–4.7, 5.0 –5.5, 5.7–6.38, 6.8–7.5, 7.75 –8.7	6.5	LCP	Flexible

https://doi.org/10.1017/S1759078724001387 Published online by Cambridge University Press

Conclusion

A flexible UWB antenna with six notched bands is proposed. The antenna employs a flexible LCP substrate, making it suitable for wearable devices. The six notched bands within the operating frequency range of 2.7–13.7 GHz are achieved through the integration of four SCRS and two symmetrical L-shaped branches. The antenna exhibits notches at 3.1–3.75 GHz, 4.14–4.7 GHz, 5–5.5 GHz, 5.7–6.38 GHz, 6.8–7.5 GHz, and 7.75–8.7 GHz, effectively suppressing interference in the WiMAX band, ARN band, WLAN downlink band, C-band uplink band, C-band/INSAT/super expansion band, and ITU-8 GHz band. The measured results confirm that the antenna successfully achieves six band-notched characteristics across its operating range and satisfactory radiation performance. Additionally, the antenna maintains robustness and flexibility under bending conditions, making it a promising candidate for wearable wireless communication systems.

Acknowledgements. The authors would like to thank the CETC Shanghai Microwave Communication Co., Ltd for providing measure facility.

Competing interests. All authors disclosed no relevant relationships.

References

1. **Rao Devana VNK, Kusuma Kumari E, S CK** (2022) A novel foot-shaped elliptically embedded patch-ultra wide band antenna with quadruple band notch characteristics verified by characteristic mode analysis. *International Journal of Communication Systems* **35**(15):e5284, 1–19.
2. **Z DC, P YZ, Y LH** (2021) Four-element CPW-Fed UWB MIMO slot antenna with high isolation and triple band-notched characteristics. *Progress In Electromagnetics Research C* **116**:145–156.
3. **Singh HS and Kalraiya S** (2018) Design and analysis of a compact WiMAX and WLAN band notched planar monopole antenna for UWB and bluetooth applications. *International Journal of RF & Microwave Computer-Aided Engineering* **28**(9):e21432.
4. **Lin H, Lu Z, Wang Z** (2023) A compact UWB monopole antenna with triple band notches. *Micromachines* **14**(3), 518.
5. **Babu PR, Ramakrishna D and Ensermu G** (2023) Triple band-notch UWB antenna embedded with slot and EBG structures. *Wireless Communications and Mobile Computing* **2023**(1):3461751.
6. **Premalatha B, Prasad MVS and Murthy MBR** (2019) Multi-band notched antennas for UWB applications. *Radioelectronics and Communications Systems* **62**:609–618.
7. **Sharma M** (2020) Design and analysis of MIMO antenna with high isolation and dual notched band characteristics for wireless applications. *Wireless Personal Communications* **112**(3):1587–1599.
8. **Deng Z, Lai C, Wang Y** (2022) Design of a quadruple band-notched ultra-wideband (UWB) antenna using curled c-shaped structures and interdigital inductance slots. *Electronics* **11**(23), 3949.
9. **P KO, Kumar P, Ali T** (2023) A quadruple notch uwb antenna with decagonal radiator and sierpinski square fractal slots. *Journal of Sensor and Actuator Networks* **12**(2), 24.
10. **Dilruba Geyikoglu M** (2023) A novel UWB flexible antenna with dual notch bands for wearable biomedical devices. *Analog Integrated Circuits and Signal Processing* **114**(3):439–450.
11. **Chilukuri S and Gogikar S** (2019) A cpw fed denim based wearable antenna with dual band-notched characteristics for uwb applications. *Progress In Electromagnetics Research C* **94**:233–245.
12. **Roy A, K BA, Nandi A** (2023) Ultra-wideband flexible wearable antenna with notch characteristics for WLAN applications. *Progress In Electromagnetics Research C* **129**:143–155.
13. **Rahmatian P, Moradi E and Movahhedi M** Single notch band UWB off-body wearable antenna with full ground plane[C]//2019 27th Iranian Conference on Electrical Engineering (ICEE). IEEE, 2019: 1228–1232.
14. **Zhao Z, Zhang C, Lu Z** (2023) A miniaturized wearable antenna with five band-notched characteristics for medical applications. *IEEE Antennas and Wireless Propagation Letters* **22**(6), 1–5.
15. **Hoosung Lee;Yong Bae Park**.Wideband ring-monopole flexible antenna with stub for WLAN/C-band/X-band applications. *Applied Sciences* **12**1 10717.
16. **Kumar CA P and Ali T** (2021) A.sharma.flexible substrate based printed wearable antennas for wireless body area networks. *Medical Applications.radioelectronics and Communications Systems* **64**(7):337–350.
17. **Chengzhu D, Wang X and Zhong S** (2022) A CPW-fed flexible ultra-wideband MIMO antenna based on liquid crystal polymer for IoT applications. *Journal of Electromagnetic Waves & Applications* **36**(15):1–13.
18. **Wang T-S, Cheng-zhuacaa D, Shu H-F and YueZhi-Huaa A** (2024) Flexible UWB slot antenna with quad band-notched characteristics for wearable application. *Progress In Electromagnetics Research C*, Vol.**140**:127–134.
19. **Du C, Li X and Zhong S** Compact liquid crystal polymer based tri-band flexible antenna for WLAN/WiMAX/5G applications. IEEE Access, 2019:1.
20. **Xiao W, Mei T, Lan Y** (2017) Triple band-notched UWB monopole antenna on ultra-thin liquid crystal polymer based on ESCSRR. *Electronics Letters* **53**(2), 57–58.
21. **Du C, Wang X, Y JG** (2021) A compact tri-band flexible MIMO antenna based on liquid crystal polymer for wearable applications. *Progress in Electromagnetics Research* **102**:217–232.

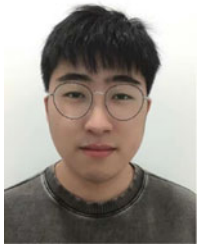

Tianshi Wang was born in Heilongjiang Province, China in 1999. He received the B.S. degree from the Shanghai University of Electric Power in 2021. He is currently pursuing the M.S degree in College of Electronics and Information Engineering, Shanghai University of Electric Power. His research interests include UWB antenna with band-notched characteristics and flexible antenna.

Chengzhu Du was born in Haikou, Hainan Province, China. She received the B.S. degree from the Xidian University, M.S. degree from Nanjing University of Posts and Telecommunications and PhD degree from Shanghai University, in 1995, 2003, and 2012, respectively, all in electromagnetic wave and microwave technology. She is currently an associate Professor of Shanghai University of Electric Power. Her research interests include flexible antenna and textile antenna, multiband and wideband antennas, and MIMO technologies.

https://doi.org/10.1017/S1759078724001387 Published online by Cambridge University Press